JACS
JOURNAL OF THE AMERICAN CHEMICAL SOCIETY

ARTICLE

pubs.acs.org/JACS

On the Mechanism of Dimethylarginine Dimethylaminohydrolase Inactivation by 4-Halopyridines

Corey M. Johnson,[†] Arthur F. Monzingo,[‡] Zhihong Ke,[§] Dae-Wi Yoon,[†] Thomas W. Linsky,[‡] Hua Guo,[*,§] Jon D. Robertus,[*,‡] and Walter Fast[*,†]

[†]Division of Medicinal Chemistry, College of Pharmacy, [‡]Department of Chemistry and Biochemistry, University of Texas, Austin, Texas 78712, United States

[§]Department of Chemistry and Chemical Biology, University of New Mexico, Albuquerque, New Mexico 87131, United States

Supporting Information

ABSTRACT: Small molecules capable of selective covalent protein modification are of significant interest for the development of biological probes and therapeutics. We recently reported that 2-methyl-4-bromopyridine is a quiescent affinity label for the nitric oxide controlling enzyme dimethylarginine dimethylaminohydrolase (DDAH) (Johnson, C. M.; Linsky, T. W.; Yoon, D. W.; Person, M. D.; Fast, W. *J. Am. Chem. Soc.* **2011**, *133*, 1553−1562). Discovery of this novel protein modifier raised the possibility that the 4-halopyridine motif may be suitable for wider application. Therefore, the inactivation mechanism of the related compound 2-hydroxymethyl-4-chloropyridine is probed here in more detail. Solution studies support an inactivation mechanism in which the active site Asp66 residue stabilizes the pyridinium form of the inactivator, which has enhanced reactivity toward the active site Cys, resulting in covalent bond formation, loss of the halide, and irreversible inactivation. A 2.18 Å resolution X-ray crystal structure of the inactivated complex elucidates the orientation of the inactivator and its covalent attachment to the active site Cys, but the structural model does not show an interaction between the inactivator and Asp66. Molecular modeling is used to investigate inactivator binding, reaction, and also a final pyridinium deprotonation step that accounts for the apparent differences between the solution-based and structural studies with respect to the role of Asp66. This work integrates multiple approaches to elucidate the inactivation mechanism of a novel 4-halopyridine "warhead," emphasizing the strategy of using pyridinium formation as a "switch" to enhance reactivity when bound to the target protein.

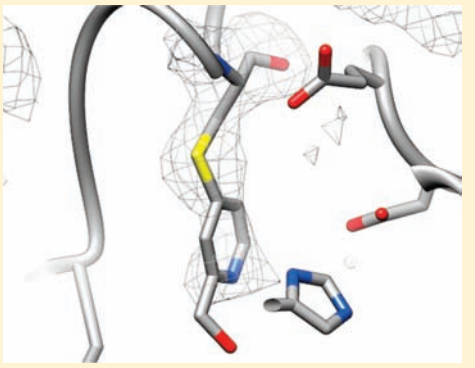

Small molecules that are capable of covalently modifying proteins are currently undergoing a type of renaissance as they are newly applied to solve problems in chemical biology and proteomics, as well as in drug design, discovery, and development.[1−3] There are a number of strategies that incorporate moderately electrophilic groups into the design of affinity-based probes, activity-based probes, and activity-based protein profiling reagents. A few noted examples include the use of electrophilic phosphonates to target serine hydrolases,[4] epoxides and electrophilic ketones (alpha halomethyl ketones and acyloxymethyl ketones) to target cysteine hydrolases,[5−8] Michael acceptors to target ubiquitin-specific proteases,[8] and alkynes to target cytochrome P450s.[9] Though typically disfavored during drug development, there are also a number of examples of existing drugs and drugs in development that rely on a covalent modification strategy to achieve their effect.[10] Although their applications are novel, many of the reactive groups used in these biologically useful compounds are well-known and have had a long history of use as protein modification reagents. Therefore, discovery and development of new protein modifying reagents compatible with biological applications are of significant interest.

During an effort to find novel inhibitors of the nitric oxide-controlling enzyme dimethylarginine dimethylaminohydrolase (DDAH),[11] 2-methyl-4-bromopyridine was discovered to be a time-dependent inhibitor.[12] Mechanistic analysis determined that this 4-halopyridine is a covalent inactivator that selectively modifies the active site Cys residue. The inactivation mechanism is most consistent with that described for quiescent affinity labels[13,14] in that the compound is relatively unreactive (quiescent) to most biological nucleophiles but demonstrates an enhanced reactivity when bound to the active site of the target enzyme. In the specific case of 2-methyl-4-bromopyridine, DDAH was proposed to selectively bind and stabilize the more reactive pyridinium form thus facilitating the inactivation process. This result was significant because, to our knowledge, 4-halopyridines had not previously been reported as covalent protein modifiers and because they likely display a selectivity different than existing reagents.

Because of the potential application of 4-halopyridines as both specific DDAH inhibitors and as more general tools in chemical

Received: April 12, 2011
Published: June 01, 2011

biology, we sought to understand their inactivation mechanism in more detail. The studies described below combine solution-based, structural, and molecular modeling approaches to investigate the mechanism of DDAH inactivation by the 4-halopyridine, 2-hydroxymethyl-4-chloropyridine (**1**). This work seeks to identify whether 4-halopyridines inactivate DDAH using a common mechanism, to provide insight into developing more selective and potent DDAH inhibitors for pathologies for which nitric oxide blocking drugs are indicated,[15] and to better understand the reactivity and selectivity of this novel modification strategy for broader applications in chemical biology.

MATERIALS AND METHODS

Materials. Unless noted otherwise, all chemicals are from Sigma-Aldrich Chemical Co. (St. Louis, MO). All enzymes, including wild type *Pseudomonas aeruginosa* DDAH and the mutants C249S, D244N, and D66N were purified and assayed as described previously.[12] Two complementary mutagenic oligonucleotides, (forward) 5′-CGACGGCGGCGTcgcTTGCATGTCGCTG-3′ and 5′-CAGCGACATGCAAgcgACGCCCCGTCG-3′ were used to introduce a S248A mutation (lowercase) in the DDAH sequence by Quikchange mutagenesis, by a previously described protocol. Synthetic DNA primers were from Sigma-Genosys (The Woodlands, TX). Rapid plasmid isolation kits were from Invitrogen (Carlsbad, CA). 2-Hydroxymethyl-4-chloropyridine (**1**) was obtained from two different sources, ChemBridge (San Diego, CA) and Sigma-Aldrich. 2-Hydroxymethylpyridine was from Sigma-Aldrich.

Time-Dependent Inactivation of DDAH. Purified recombinant DDAH (29 μM) was incubated with KCl (100 mM) and **1** (0.150−3 mM) in K_2HPO_4 buffer (100 mM) and EDTA (0.05 mM) at pH 7.5, 25 °C. Some experiments also included a prior incubation (1 h) of **1** with excess glutathione (5 mM) before addition of enzyme to initiate the inactivation. Aliquots were removed from the enzyme-containing incubations at various time points (0−80 min) and diluted 100-fold into an assay solution containing excess (1 mM) substrate N^{ω}, N^{ω}-dimethyl-L-arginine. The remaining enzyme activity was assayed as described previously,[12] using a color-developing reagent (COLDER)[16] to derivatize the urea group of the L-citrulline product. Briefly, COLDER (200 μL) was added to each 100 μL reaction in a 96-well plate and incubated for 15 min at 95 °C. Samples were cooled for 20 min at 25 °C, and the absorbance at 540 nm was determined for each well using a Perkin-Elmer (Waltham, MA) VICTOR^{3}V 1420 multilabel counter plate reader. The observed inactivation rates (k_{obs}) were determined by fitting the percent remaining activity over time to a single-exponential equation. The resulting k_{obs} values were then plotted against inactivator concentration. No saturation was observed, so these were fitted with a linear equation to determine the second order inactivation rate constant (k_{inact}/K_I). All fits were calculated using KaleidaGraph (Synergy Software, Reading, PA).

Mass Spectrum Analysis of Inactivated DDAH and DDAH Mutants. To characterize any covalent adducts formed with the enzyme during inactivation, 90 min incubations of **1** or **2** (1 mM each) with wild type and mutant DDAH variants were carried out under similar conditions to those described above. Because of the high concentration of enzyme, incubations were not acid quenched in order to avoid precipitation. To control for acid-quenched conditions, alternative samples were prepared using lower concentrations of enzyme (2 μM) in the incubation mixtures and then acid quenched using trifluoroacetic acid (TFA, 6 N) previous to MS analysis, and this gave consistent results. Samples were analyzed by ESI-MS on a ThermoFinnigan LCQ (San Jose, CA) ion trap mass spectrometer as described previously.[12]

Synthesis of 1-Methy-4-chloro-2-hydroxymethylpyridine (2). A solution of **1** (0.1077 g, 0.75 mmol) in 4 mL of CH_2Cl_2 was treated with CH_3I (0.456 g, 3.21 mmol), and the reaction mixture was stirred overnight at 25 °C. The resulting precipitate was collected by vacuum filtration, washed with CH_2Cl_2 (30 mL), and dried under high vacuum to yield **2**. ^{1}H NMR (400 MHz, DMSO-d_6) δ 8.86 (d, J = 6.8 Hz, 1H, Ar−H), 8.29 (d, J = 2.1 Hz, Ar−H), 8.06 (dd, J = 9.2 Hz, J = 2.4 Hz, 1 H, Ar−H), 4.97 (s, 2H, CH_2), 4.23 (s, 3H, N−CH_3); HRMS CI mass calculated for C_7H_9ClNO 158.0373, found 158.0371.

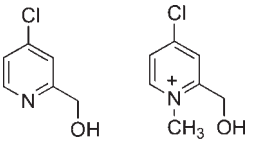

(**1**) (**2**)

Crystallization and Data Collection. Purified *P. aeruginosa* DDAH was incubated with **1** by mixing 500 μL of DDAH (288 μM) in the final purification buffer[12] with 30 μL of a stock solution of compound **1** (20 μM) in DMSO. The mixture was concentrated to approximately 14 mg/mL DDAH (470 mM) using a Microcon YM-10 centrifugal filter device (Millipore, Billerica, MA).

The protein−inhibitor complex was crystallized at 25 °C using the hanging drop method from 20% PEG 3350, pH 7.1, 0.2 M ammonium acetate. Prior to data collection, crystals were treated with cryoprotectant by transferring to 30% PEG 3350, 0.1 M HEPES, pH 7.2, 0.2 M ammonium acetate for 1−5 s. A crystal, mounted in a cryoloop (Hampton Research, Laguna Niguel, CA), was frozen by dipping in liquid nitrogen and placed in the cold stream on the goniostat.

X-ray diffraction data were collected from the crystal at 100 K on an RAXIS IV++ image plate detector (Rigaku, The Woodlands, TX) with X-rays generated by a Rigaku MicroMax-007 HF rotating anode generator operated at 40 mV, 30 mA. Diffraction images were processed and data reduced using HKL2000.[17]

Structure Determination and Analysis. The crystal cell parameters indicated that the asymmetric unit likely contained two DDAH molecules. MOLREP,[18] from the CCP4 suite,[19] was used to determine the molecular replacement solution for the two DDAH molecules in the asymmetric unit, using the *P. aeruginosa* DDAH C249S structure (PDB accession code 1H70)[20] as the model.

Model building was done using Coot.[21] Refinement of models was performed with the Crystallography and NMR System (CNS) (Version 1.21) using the slow-cooling protocol.[22] There were several rounds of refinement followed by rebuilding of the model. To facilitate manual rebuilding of the model, a difference map and a $2F_o-F_c$ map, SIGMAA-weighted to eliminate bias from the model,[23] were prepared. A portion (5%) of the diffraction data were set aside throughout refinement for cross-validation.[24] Molprobity[25] was used to determine areas of poor geometry. Coot was used to locate bound solvent molecules from peaks of height 3.5 standard deviations above the mean in a difference map and that were within 3.5 Å of a protein nitrogen or oxygen atom. Potential water sites were reviewed manually using Coot. Computations were done on an HP Pavilion a6700z computer (Hewlett-Packard Co., Palo Alto, CA).

Atomic Coordinates. Coordinates of the refined model of *P. aeruginosa* DDAH after inhibition by compound **1** have been deposited in the Protein Data Bank with entry code 3RHY.

Molecular Modeling. By using the X-ray crystal structure of *P. aeruginosa* DDAH (PDB code 1H70)[20] with ligands and waters removed, **1** was docked to the active site using Autodock 4.2.[26] The active site was defined by a box that extended at least 8 Å on all sides from the crystallographic ligand (L-citrulline). The Lamarckian genetic algorithm was used as the search method to generate 10 poses with a population size of 150, mutation rate of 0.02, and 25 000 000 energy evaluations per run. A representative pose from the largest cluster was chosen as a starting point for simulations described below.

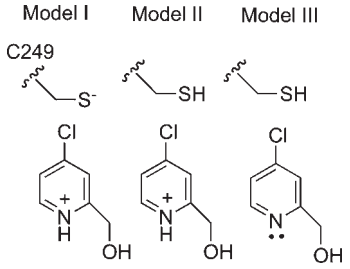

Figure 1. Illustration of the three protonation models used in molecular dynamics.

To test the protonation states of the active site cysteine residue and the inactivator, three models were investigated in the current study, as shown in Figure 1. In both models I and II, the inhibitor is protonated while the cysteine is either deprotonated (I) or protonated (II). In model III, both cysteine and inhibitor are neutral. The initial structures of the three models were all based on the docked pose described above. Hydrogen atoms were added using Leap in Amber,[27] in such a fashion consistent with the local hydrogen bond network.

For each model, a 3 ns classical molecular dynamics (MD) simulation was carried out to equilibrate the solvated enzyme−inhibitor complex, which was prepared by solvating the initial structure into a periodic rectangular water box of the size approximately 77 × 72 × 69 Å^3 and then neutralizing by Na^+ ions (the amount of Na^+ ions is different from model to model). The AMBER99SB force field[28,29] and the TIP3P water model[30] were employed. Force field parameters for the inhibitor were prepared using Antechamber in Amber,[27] and its charge was fitted using the RESP method.[31] Throughout the MD simulations, periodical boundary conditions were used. Long-range electrostatic interactions were treated with particle mesh Ewald (PME) method,[32,33] while a 8 Å cutoff was introduced for nonbonding interactions. The SHAKE algorithm[34] was applied for all covalent bonds involving hydrogen. All MD simulations were carried out with the Amber package. The same protocol was used for the product complexes.

All quantum mechanical/molecular mechanical (QM/MM) calculations were conducted with modified versions of the QChem[35] and TINKER programs.[36] Throughout the QM/MM minimization and QM/MM MD simulations, the QM subsystem was treated at the B3LYP/6-31G(d) level. The MM atoms were described with AMBER99SB force field[28,29] and the TIP3P water model.[30] The QM−MM boundaries were treated with the pseudobond approach.[37] Spherical boundary conditions were applied so that only atoms inside of 20 Å of the reaction center were free to move.

By using the final snapshots from classical MD simulations, the QM/MM models were prepared by removing water molecules outside of a sphere 27 Å from the origin, which is defined by the Cl position of the inhibitor. For model I, the QM subsystem consists of the inhibitor molecule and the side chains of His162 and Cys249, while for the other two models, the QM subsystem is composed of the inhibitor molecule and the side chains of Glu65, Ser248, and Cys249. These systems were minimized using the QM/MM Hamiltonian. In addition, a 5 ps QM/MM MD run was performed to equilibrate the system under the same QM/MM Hamiltonian for model I and model II.

The reaction paths were mapped out using the reaction coordinate driving (RCD) method[38] on putative reaction coordinates. The free-energy profile of a reaction is given by the potential of mean force (PMFs) along the reaction coordinate. This was accomplished using the umbrella sampling method[39] with 20 windows. In each window, a 10 ps QM/MM MD simulation was performed using harmonic bias potentials with force constants ranging from 30 to 100 kcal/mol Å^2. The Berendsen thermostat[40] was used to control the system temperature at 300 K. The final PMF was calculated with the weighted histogram analysis method (WHAM).[41] The QM/MM method used here is essentially the same as in our recent publication on arginine deiminase,[42] which is a member of the same enzyme superfamily as DDAH and is believed to have a similar catalytic mechanism.[43,44]

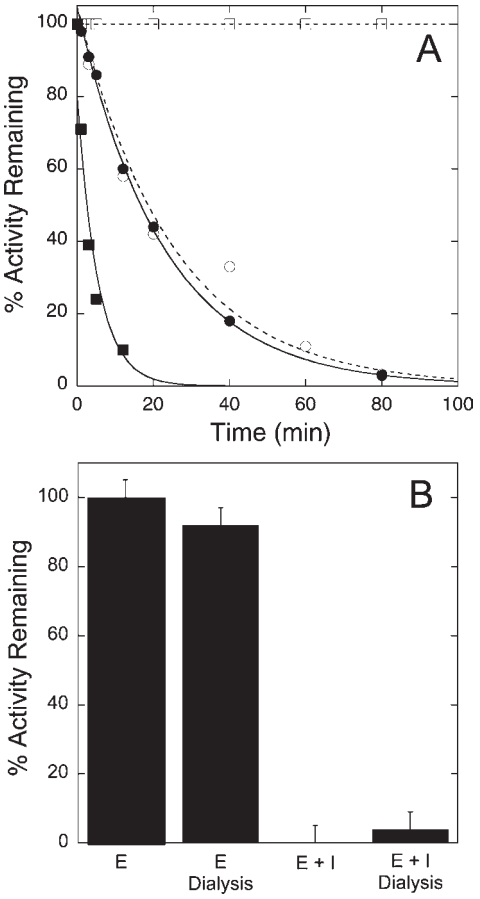

Figure 2. Time-dependent inhibition of DDAH by inactivators **1** and **2**. (A) Time-dependent loss in DDAH activity is observed after incubation with **1** (●, 1 mM) and **2** (■ 1 mM), solid lines. Each experiment is then repeated after addition of a preincubation (1 h) of each inactivator with glutathione (5 mM) before monitoring time-dependent loss of DDAH, dashed lines. The glutathione preincubation with **1** (○) does not significantly effect the observed inactivation rate, but glutathione preincubation with **2** (□) completely blocks the ability of this compound to inactivate DDAH. (B) Enzyme inactivated by **1** was dialyzed overnight and assayed for recovery of activity ("E" is an enzyme only control; "E dialysis" is enzyme only after dialysis; "E + I" is inactivated enzyme; "E + I dialysis" is inactivated enzyme after dialysis).

RESULTS AND DISCUSSION

We recently reported the discovery of 2-methyl-4-bromopyridine as a novel quiescent affinity label that covalently modifies the active site Cys of DDAH.[12] To our knowledge, there are no other reports of halopyridines that covalently modify proteins, so we sought to understand this process in more depth by using multiple approaches—solution studies, X-ray crystallography, and molecular modeling—to characterize the mechanism of DDAH inactivation by the related compound 2-hydroxymethyl-4-chloropyridine (**1**).

Solution Studies. In an attempt to generalize the results obtained with 2-methyl-4-bromopyridine to other 4-halopyridines, the following experiments were undertaken to determine

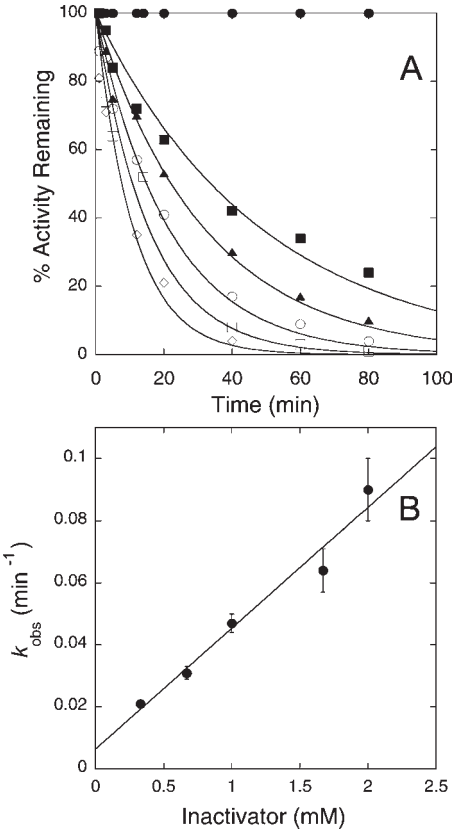

Figure 3. Time- and concentration-dependent inactivation of DDAH by **1** at pH 7.5 (A) Exponential fits (solid lines) to the observed inactivation of DDAH at pH 7.5, 25 °C by different concentrations of **1**: 0 (●), 330 μM (■), 670 μM (▲), 1 mM (□), 1.67 mM (○), 2 mM (◇). (B) Concentration dependence of the pseudofirst-order k_{obs} values give a second order rate constant of 0.65 ± 0.07 M^{-1} s^{-1} for inactivation. The observed *y*-intercept is 0.006 ± 0.005 min^{-1}.

whether **1** uses a similar inactivation mechanism. In agreement with our previous report,[12] incubation of **1** with *P. aeruginosa* DDAH was found to result in time-dependent inhibition that could not be blocked by preincubation with glutathione (Figure 2A). Therefore, **1** is not considered to be a reactive compound under these conditions. Inhibition cannot be reversed by dilution into excess substrate or by dialysis, and so, it is characterized as an irreversible inactivation (Figure 2B). Extended dialysis times also did not result in any regained activity (Figure S1 of the Supporting Information). The observed rates of inactivation do not saturate with increasing inactivator concentrations up to 2 mM and are well described by a second order rate constant of 0.65 ± 0.07 M^{-1} s^{-1} at pH 7.5, 25 °C (Figure 3). This inactivation rate constant is 7-fold less than that of 2-methyl-4-bromopyridine[12] under the same conditions (4.8 M^{-1} s^{-1}), the difference of which can be ascribed either to the addition of the 2′ hydroxyl group or, more likely, to the substitution of chlorine for bromine. As with 2-methyl-4-bromopyridine, the protonated pyridinium form of **1** is expected to be the inactivating species. However, because the predicted pK_a value[45] of **1** is 3.6, only a small concentration of the more reactive pyridinium ion is present in bulk solution at pH 7.5, consistent with the stability of this compound toward preincubation with physiological concentrations of glutathione (Figure 2A) and with the lack of saturation kinetics in inactivation rates (Figure 3). Complete formation of the more reactive pyridinium form can be enforced by synthesis of *N*-methyl-2-hydroxymethyl-4-chloropyridine (**2**), which is observed to inactivate DDAH at a rate that is greater than that of **1** when assayed at the same concentration (Figure 2A). However, preincubation with glutathione blocks all inactivation by **2**, indicating that *N*-methylation renders the compound too reactive for selective use in a complex thiol-containing biological milieu (Figure 2A). The chloro substituent is found to be essential for inactivation, and addition of excess substrate to the preincubation mixtures slows the observed inactivation rate, consistent with covalent modification occurring at the active site of DDAH (Figure S2 of the Supporting Information). Inactivation does not occur after release of a reactive species from the active site (metabolic activation) because a second aliquot of fresh enzyme added to the preincubation mixture is not inactivated with a faster observed rate (Figure S3 of the Supporting Information).

Because the DDAH active site environment plays a crucial role in the inactivation mechanism, a number of mutations were tested for reactivity with **1**. Cys 249 and His162 are the active site nucleophile and a general acid/general base, respectively, that participate in the normal catalytic mechanism. Both of these residues have been shown to be susceptible to covalent modification.[46,47] Also, the positively charged guanidinium of the substrate binds to the carboxylate-rich active site. To determine if any active site carboxylates found within 8 Å of Cys 249 participate in binding the pyridinium form of the inactivator, site-directed mutants were prepared for Glu65, Asp66, and Asp244. Wild type and D244N DDAH variants both form covalent adducts upon incubation with **1**, showing mass additions (105 and 107 ± 10 Da, respectively) that are consistent with covalent attachment of one equivalent of hydroxymethylpyridine to each enzyme (Table 1). These results also indicate that Asp244 is not essential for covalent modification to occur. In contrast, the C249S and D66N DDAH variants are both incapable of forming a covalent adduct when incubated with **1** (Table 1). These results are consistent with a covalent inactivation mechanism in which Asp66 stabilizes the more reactive pyridinium form of **1**, which accepts attack by Cys249 with subsequent loss of a chloride ion. One notable difference from our prior study[12] is that the D66N mutation can completely block enzyme modification by **1**, indicating that this active site interaction is even more essential for inactivation by **1** than for the related bromopyridine, for which this mutation only provides a partial block. As predicted, the covalent modification reaction that is blocked by the D66N mutation can be "rescued" by substitution of the *N*-methylated analogue (**2**) and leads to complete modification of DDAH under the same experimental conditions. This result is consistent with our hypothesis that Asp66 functions to stabilize the pyridinium form of the halopyridine inactivator. In summary, all of the solution studies support the proposal that the inactivation mechanism proposed for 2-methyl-4-bromopyridine can be generalized to include compound **1** and likely other 4-halopyridines.

Structural Studies. Since the active site environment of DDAH plays a significant role in the inactivation mechanism, we sought to determine the X-ray crystal structure of the inactivated complex. Crystals were obtained from a mixture of the *P. aeruginosa* DDAH protein and compound **1** and belong to space group $P2_12_12_1$ with cell constants, a = 45.8, b = 73.3, c = 149.5 Å. There are two molecules per asymmetric unit, giving a V_m of 2.2 $Å^3$/Da. Crystallographic data for the complex of

Table 1. Summary of Deconvoluted Protein Masses Observed in ESI-MS Spectra of Control and Inactivated DDAH

		control incubations with no inactivator	incubations with **1**		incubations with **2**	
DDAH preparation	theoretical calcd mass (Da)	observed mass (Da)[a]	observed mass (Da)[a]	mass difference (Da)	observed mass (Da)[a]	mass difference (Da)
wild type	30 503	30 498	30 603	105	30 617	119
C249S	30 487	30 481	30 481	0	ND[b]	ND[b]
D66N	30 502	30 495	30 493	−2	30 615	120
D244N	30 502	30 496	30 603	107	30 617	121
S248A	30 487	30 482	30 588	106	30 603	121

[a] The deconvoluted ESI-MS spectra are reported with errors of ±10 Da. [b] Not determined.

Table 2. Crystallographic Data

	DDAH−compound **1**
space group	$P2_12_12_1$
cell constants	45.8, 73.3, 149.5 Å
resolution (Å)[a]	50.−2.18 (2.22−2.18)
R_{merge} (%)[a]	0.075 (0.462)
$\langle I/\sigma_I \rangle$[a]	10.1 (3.3)
completeness (%)[a]	99.1 (98.4)
unique reflections	27 154
redundancy	7.0
no. of residues	496
no. of protein atoms	3882
no. of ligand atoms	16
no. of solvent atoms	227
$R_{working}$	0.209
R_{free}	0.265
average B factor for protein atoms (Å^2)	36.0
average B factor for ligand atoms (Å^2)	54.2
average B factor for solvent atoms (Å^2)	39.1
rms deviation from ideality	
bonds (Å)	0.006
angles (°)	1.319
Ramachandran plot	
% of residues in most favored region	96.7
% of residues in additional allowed region	3.3

[a] Values in parentheses correspond to highest-resolution shell.

compound **1** and *P. aeruginosa* DDAH are summarized in Table 2. A Ramachandran plot shows 96.7% of residues in the most favorable region and 3.3% in additional allowed space. As observed previously, DDAH crystallized as a dimer with 3-strand β-sheets from each monomer bonding together in an antiparallel manner, producing a 6-strand β-sheet. The complete refined model includes two covalently bound adducts and 227 solvent molecules.

With two notable exceptions, the DDAH structure is virtually identical to the previously determined *P. aeruginosa* DDAH C249S[20] and H162G[48] structures with a root-mean-square deviation (rmsd) of 0.4 Å for equivalent Cα atoms. One contrasting feature is a loop near the active site, residues 17−22, that is typically stabilized by hydrogen bonds to the amino acid moiety of substrate-like ligands that are bound at the active site. In the structure of DDAH after inactivation by **1**, the

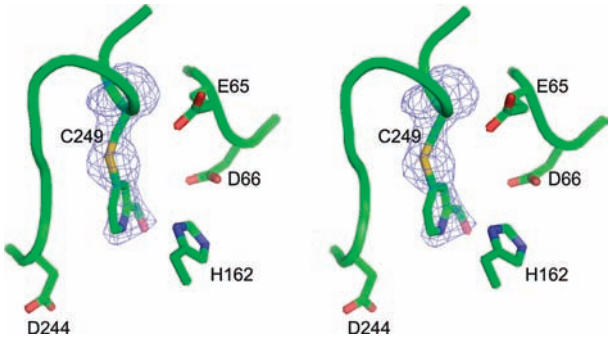

Figure 4. Inhibitor covalently bound in the active site. A 2.18 Å F_o-F_c omit map shows continuous electron density for the bound inhibitor and residue Cys249 in the active site of DDAH. The map is contoured at 3 σ, and the model is shown as a divergent stereo image.

17−22 loop is instead disordered, reflecting the inability of **1**, which lacks an amino acid moiety, to provide sufficient stabilizing interactions. The second notable difference is obviously the presence of a different ligand at the active site. Following molecular replacement of the two molecules, a difference electron density map with Cys249 omitted clearly shows strong, continuous density between the Cys residue and the active site ligand (Figure 4). This connection is consistent with covalent bond formation and the remaining extra electron density is consistent with that expected for the 2-hydroxymethylpyridine adduct. The pyridine ring is placed adjacent to Phe63, approximately in the same site predicted for the hydrophobic portion of the substrate (N^{ω},N^{ω}-dimethyl-L-arginine) side chain. This result corroborates the conclusions regarding inactivation at Cys249 based on the solution studies above and provides additional information about ligand placement.

However, no interaction is observed between the inactivator and Asp66. Through mutational analysis, Asp66 was proposed to stabilize the protonated pyridinium form of the inactivator. In contrast, the structural model shows that the pyridine nitrogen does *not* directly contact *any* protein residue. There is likely some conformational diversity of the adduct because no density is apparent for the 2-hydroxymethyl moiety of the inactivator, suggesting that the pyridine ring may rotate about the N−S bond formed with Cys249. Even so, this rotation would not enable a direct interaction with the side chain of Asp66. Therefore, the structural data do not provide support for the proposed role of this residue.

Molecular Modeling. There are obvious confirmatory findings between the structural and solution studies, primarily the specific formation of a covalent adduct at the active site Cys residue. However, the structural studies do not show the proposed interaction between the inactivator and Asp66. Therefore, we sought to use molecular modeling to provide more information about the inactivation mechanism and how it relates to the structure of the final inactivated species. Because a variety of different starting protonation states are plausible for the enzyme and inactivator, three models were queried using molecular modeling (Figure 1). Model I includes a deprotonated Cys249 thiolate and the protonated pyridinium form of compound **1**. Model II includes a protonated neutral Cys249 thiol and the protonated pyridinium form of compound **1**. Model III starts with a protonated neutral Cys249 thiol and the neutral form of compound **1**.

Classical MD simulations of models I, II, and III revealed little structural change to the DDAH enzyme, with rmsd of 1.11 ± 0.06, 1.02 ± 0.06, and 1.37 ± 0.09 Å, respectively. However, the deprotonated ligand (**1**) in model III was found to be quite floppy in the active site cavity, apparently due to the lack of a hydrogen bond between Asp66 and the inactivator. In contrast, the protonated form of **1** in models I and II is anchored tightly with a hydrogen bond to the carboxylate of Asp66, as evidenced by the H−$O_{\delta 2}$ distances of 1.95 ± 0.32 and 1.85 ± 0.16 Å, respectively.

QM/MM MD simulations of model I led spontaneously to the nucleophilic attack of the thiolate nucleophile to C_4 (namely, the chlorine-bonding carbon in the inactivator) within the first picosecond. The departure of the chloride ion is concerted with the formation of the S−C bond. This observation indicates that the reaction at this protonation state is barrierless at room temperature, which is consistent with the strong nucleophilicity of the thiolate. However, in the resting enzyme, the side chain of Cys249 has a pK_a value of approximately 8.8 and so is predominately found in its neutral form at the inactivation pH values of 7.5 and 5.0. Therefore, if inactivation does proceed through model I, it would represent a reaction between the minor deprotonated fraction of Cys249 with the minor protonated fraction of **1**.

In contrast, the active site of ligand-bound DDAH is stable in model II during the QM/MM MD runs, which suggests the existence of a reaction barrier. Using the last snapshot of the QM/MM MD trajectory, we performed RCD calculations using the following reaction coordinate: $\xi = -d(H_\gamma(C249) - O_\gamma(S248)) - d(S_\gamma(C249) - C_4(\text{inactivator}))$. This definition was determined after examining several possible proton transfer routes. Specifically, it depicts the deprotonation of the thiol group of Cys249 by Glu65 via Ser248. Our choice of Glu65 as the proton acceptor is motivated by its location and the experimental observation that its mutation leads to a loss in activity.[12] We also mapped out a reaction path for model III that uses the same reaction coordinate. Because of the floppy nature of deprotonated **1**, the initial structure was prepared by starting with the structure of model II and then removing the proton from the pyridine's nitrogen.

The calculated energy profile for model III (not shown) indicated a barrier of approximately 35 kcal/mol, significantly higher than that of model II, which is only approximately 25 kcal/mol. Additionally, no stable products could be found for model III. Therefore, these observations suggest that the reaction involving deprotonated **1** is disfavored. This result is consistent with small molecule studies showing a greatly enhanced reactivity of the positive pyridinium forms of 4-halopyridines (e.g., 10^3 to 10^9-fold increase) when compared to their corresponding neutral forms.[49,50] This result is also consistent with those described above showing enhanced reactivity by the *N*-methylated pyridinium analogue **2**, the pH-dependent studies of DDAH inactivation by 2-methyl-4-bromopyridine reported earlier,[12] and the relative stability of both 4-halopyridines when incubated with excess glutathione. Taken together, these results emphasize that an important aspect of using 4-halopyridines as enzyme inactivators is the strategy of using pyridinium formation as a "switch" to enhance reactivity.

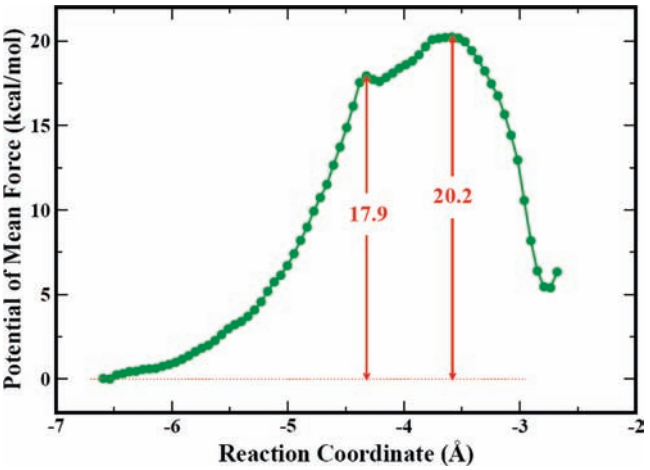

Figure 5. Calculated free energy profile for model II.

Therefore, we focused on the PMF for model II, in which both Cys249 and **1** are protonated. The resulting free energy profile shown in Figure 5 indicates a shallow intermediate flanked by two transition states, whose geometries are displayed in Figure 6. The first transition state (I), which has a lower free energy, stems essentially from the deprotonation of the Cys nucleophile, as evidenced by the H−S distance of 1.42 ± 0.04 Å. In the mean time, the Ser248 proton is en route to Glu65. The partially deprotonated Cys nucleophile is positioned for addition to the inactivator's C_4, with a S−C_4 distance of 2.81 ± 0.08 Å. The second and rate-limiting transition state (II) features the nucleophilic addition of the thiolate to the inactivator's C_4, with a S−C_4 distance of 2.50 ± 0.10 Å. At this time, the proton transfer to Glu65 is complete, and the chloride leaving group is departing. The small (2.6 kcal/mol) barrier for the thiolate nucleophilic addition is consistent with the spontaneous reaction observed with model I. The resulting overall free energy barrier of activation for the inactivation process is calculated to be 20.2 kcal/mol.

The possible relevance of Glu65 to inactivation has been established in our earlier experiment, in which the E65Q mutant disrupted both substrate turnover and protein modification by a halopyridine inactivator.[12] To experimentally test the predicted importance of Ser248 for deprotonation of Cys249, we prepared and characterized a S248A mutant of DDAH. However, this variant is still capable of substrate turnover and is still inactivated by **1** with a second order inactivation rate constant that is approximately 2-fold less than wild type DDAH (data not shown). Because of the small difference in inactivation rate constants, this preliminary experiment does not strongly support the proposed pathway. It also does not rule out the pathway because a water molecule could potentially substitute for the missing hydroxyl side chain or because there may be multiple

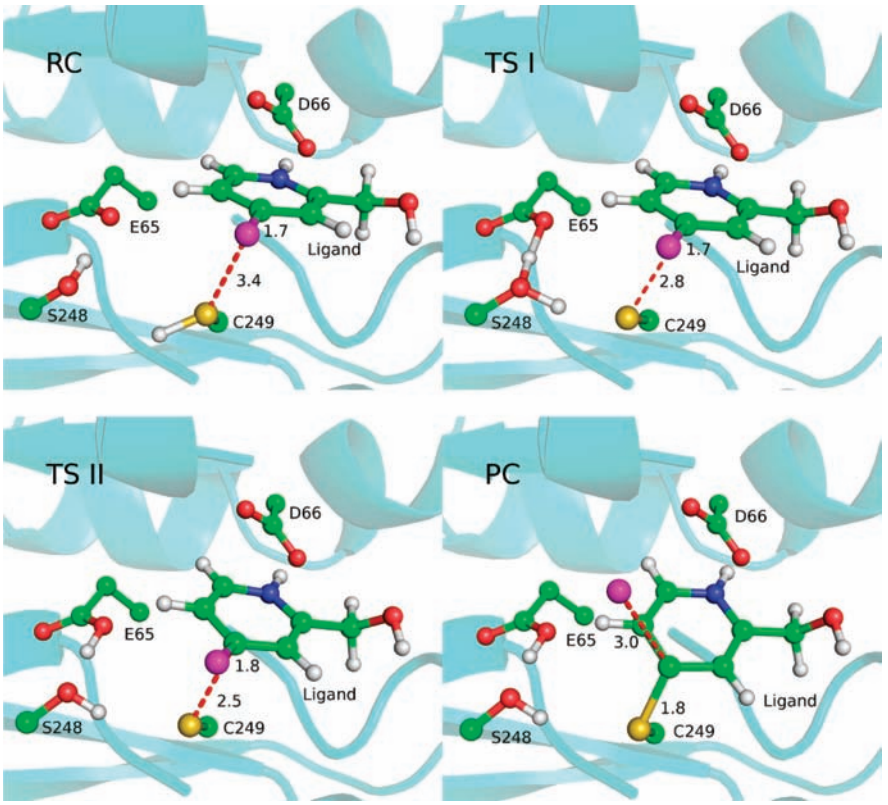

Figure 6. Illustration of the structures of reactant complex (RC), transition states (TS), and the covalent product complex (PC). The protein's ribbon depiction is in light blue, and H, C, N, O, S, and Cl atoms are in white, green, dark blue, red, yellow, and purple, respectively.

coexisting deprotonation pathways. Therefore, the proton shuttling pathway is presented here as a mechanistic proposal based on molecular modeling results and remains under study with respect to its role in both inactivation and substrate turnover mechanisms.

Molecular modeling also provides insight into the inactivator's conformation observed in the X-ray crystal structure. Since the typical pK_a values of 4-halopyridines (and 4-alkylthiopyridines as models of the inactivated enzyme) are expected to be low (<5),[45] we suspected that the final adduct observed in the structure may represent a deprotonated species. Therefore, we conducted additional MD simulations to test this hypothesis. The initial structure for these studies was prepared by starting with the inactivated product complex resulting from model II and then removing the chloride ion product. The covalent adduct was then manually deprotonated by removing the proton from the pyridine nitrogen. Starting with this initial structure, the subsequent MD trajectory showed a large conformational change of the pyridine group, which moves significantly away from the Asp66 side chain after its deprotonation. The final stable conformation in the simulation is strikingly similar to that observed for the adduct in the X-ray crystal structure (Figure 7). Meanwhile, the B factors for residues 17−22 also support the structural studies. Our MD simulations of the deprotonated hydroxymethylpyridine covalently connected with DDAH indicated that these residues are highly mobile, as evidenced by the averaged B factor for residues 17−22 of 165.3 Å^2, much larger than 23.7 Å^2 observed for DDAH bound with the substrate (N^{ω}, N^{ω}-dimethyl-L-arginine). Therefore, these results support a final deprotonation step in the inactivation mechanism. We note that deprotonation of the adduct leaves a neutral pyridine that would be less reactive toward hydrolysis, increasing its stability and enforcing the irreversibility of inactivation.

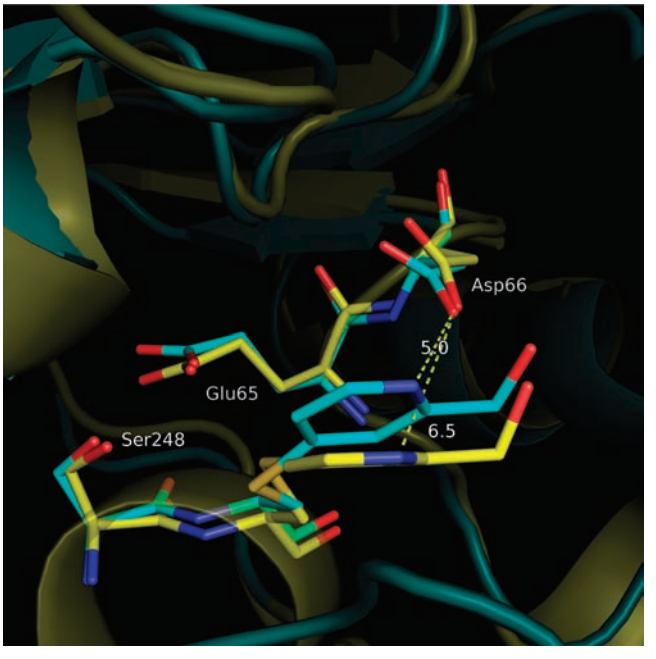

Figure 7. Comparison between the snapshot taken from the MD simulation (yellow) and the X-ray structure (blue) of the inactivator−enzyme complex.

In summary, an integrated approach using solution-based, structural, and molecular modeling studies was used to probe

Scheme 1

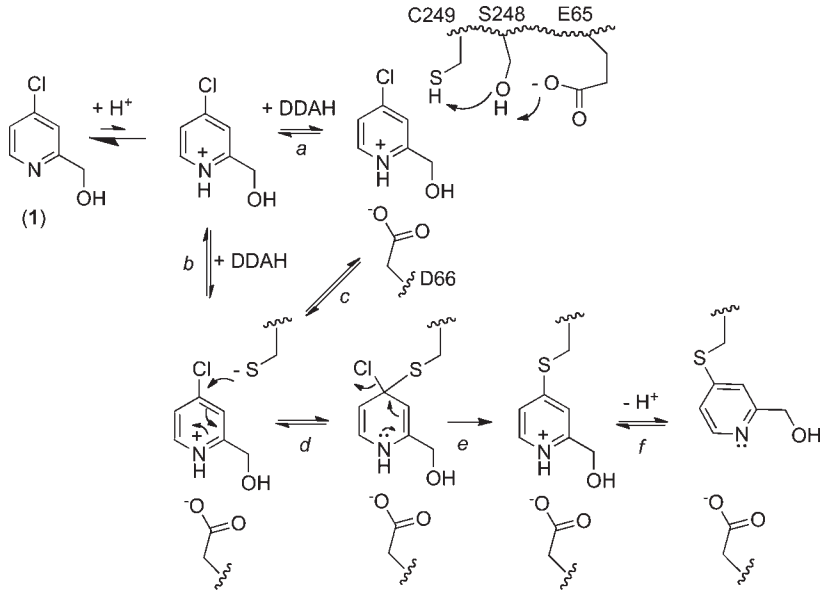

the mechanism of DDAH inactivation by **1** and supports the following proposal (Scheme 1): In solution, **1** is found predominately in its less reactive neutral form and so remains unreactive (quiescent) toward biological nucelophiles such as glutathione. The active site residue Asp66 binds and stabilizes the more reactive pyridinium form of the inactivator. The resting pK_a of Cys249 is approximately 8.8.[51] Therefore, binding could presumably occur to either the minor fraction of the enzyme containing an anionic Cys249 thiolate (path b) or to the predominant fraction, which contains a neutral Cys249 thiol (path a). Cys249 deprotonation, possibly facilitated by Ser248 and Glu65 residues (path c), leads to attack on C_4 of the inactivator (path d). The pyridinium form of the inactivator allows stabilization of the subsequent tetrahedral sigma-complex, which is followed by elimination of the chloride ion (path e). Lastly, deprotonation of the covalent adduct and movement away from the Asp66 side chain (path f) results in the final conformation observed in the X-ray crystal structure. This inactivation mechanism parallels that proposed for 2-methyl-4-bromopyridine and suggests that 4-halopyridine-based quiescent affinity labels may share key features in their inactivation mechanisms, namely, (1) the low pK_a of the 4-halopyridine ensures that it is predominantly neutral and unreactive in solution, (2) an active site group (Asp66 in DDAH) stabilizes the more reactive pyridinium form, and (3) an appropriately placed nucleophile (Cys 249 in DDAH) can subsequently attack, forming an irreversible adduct upon loss of the halide. The X-ray crystal structure of the final complex shows that the DDAH active site can likely accommodate further elaboration of the core halopyridine structure, suggesting that more potent and selective inactivators can be synthesized using this "warhead." Additionally, we note that the active site constraints of having a nucelophile placed at a suitable distance and orientation from a pyridinium-stabilizing group are not likely unique to DDAH, suggesting that the 4-halopyridine warhead may be useful for a much wider array of applications in the design of molecular probes, enzyme inhibitors, and therapeutics.

■ ASSOCIATED CONTENT

Supporting Information. Three figures showing tests for irreversibility of inactivation, substrate protection, halogen dependence, and metabolic activation of **2**, and a full author list for ref 35. This material is available free of charge via the Internet at http://pubs.acs.org.

■ AUTHOR INFORMATION

Corresponding Author
WaltFast@mail.utexas.edu; jrobertus@cm.utexas.edu; hguo@unm.edu

■ ACKNOWLEDGMENT

This work was supported in part by grants from the National Institutes of Health (GM69754 to W.F., AI075509 to J.D.R., and AI071992 to H.G.), the Robert A. Welch Foundation (F-1572 to W.F. and F-1225 to J.D.R.), a seed grant from the Texas Institute for Drug and Diagnostic Development (TI-3D: Welch Foundation Grant No. H−F-0032) and by the College of Natural Sciences support to the Center for Structural Biology.

■ REFERENCES

(1) Sadaghiani, A. M.; Verhelst, S. H.; Bogyo, M. *Curr. Opin. Chem. Biol.* **2007**, *11*, 20.
(2) Cravatt, B. F.; Wright, A. T.; Kozarich, J. W. *Annu. Rev. Biochem.* **2008**, *77*, 383.
(3) Heal, W. P.; Dang, T. H.; Tate, E. W. *Chem. Soc. Rev.* **2011**, *40*, 246.
(4) Simon, G. M.; Cravatt, B. F. *J. Biol. Chem.* **2010**, *285*, 11051.
(5) Hang, H. C.; Loureiro, J.; Spooner, E.; van der Velden, A. W.; Kim, Y. M.; Pollington, A. M.; Maehr, R.; Starnbach, M. N.; Ploegh, H. L. *ACS Chem. Biol.* **2006**, *1*, 713.
(6) Faleiro, L.; Kobayashi, R.; Fearnhead, H.; Lazebnik, Y. *EMBO J.* **1997**, *16*, 2271.

(7) Kato, D.; Boatright, K. M.; Berger, A. B.; Nazif, T.; Blum, G.; Ryan, C.; Chehade, K. A.; Salvesen, G. S.; Bogyo, M. *Nat. Chem. Biol.* **2005**, *1*, 33.
(8) Borodovsky, A.; Ovaa, H.; Kolli, N.; Gan-Erdene, T.; Wilkinson, K. D.; Ploegh, H. L.; Kessler, B. M. *Chem. Biol.* **2002**, *9*, 1149.
(9) Wright, A. T.; Cravatt, B. F. *Chem. Biol.* **2007**, *14*, 1043.
(10) Singh, J.; Petter, R. C.; Baillie, T. A.; Whitty, A. *Nat. Rev. Drug Discovery* **2011**, *10*, 307.
(11) Pope, A. J.; Karuppiah, K.; Cardounel, A. J. *Pharmacol. Res.* **2009**, *60*, 461.
(12) Johnson, C. M.; Linsky, T. W.; Yoon, D. W.; Person, M. D.; Fast, W. *J. Am. Chem. Soc.* **2011**, *133*, 1553.
(13) Krantz, A. *Bioorg. Med. Chem. Lett.* **1992**, *2*, 1327.
(14) Krantz, A. *Adv. Med. Chem.* **1992**, *1*, 235.
(15) Leiper, J.; Nandi, M. *Nat. Rev. Drug Discovery* **2011**, *10*, 277.
(16) Knipp, M.; Vasak, M. *Anal. Biochem.* **2000**, *286*, 257.
(17) Otwinowski, Z.; Minor, W. *Methods Enzymol.* **1997**, *27*, 307.
(18) Vagin, A.; Teplyakov, A. *J. Appl. Crystallogr.* **1997**, *30*, 1022.
(19) Collaborative Computational Project, Number 4 (CCP4) *Acta Crystallogr.* **1994**, *D5*, 760.
(20) Murray-Rust, J.; Leiper, J.; McAlister, M.; Phelan, J.; Tilley, S.; Santa Maria, J.; Vallance, P.; McDonald, N. *Nat. Struct. Biol.* **2001**, *8*, 679.
(21) Emsley, P.; Lohkamp, B.; Scott, W. G.; Cowtan, K. *Acta Crystallogr., Sect. D: Biol. Crystallogr.* **2010**, *66*, 486.
(22) Brunger, A. T.; Adams, P. D.; Clore, G. M.; DeLano, W. L.; Gros, P.; Grosse-Kunstleve, R. W.; Jiang, J. S.; Kuszewski, J.; Nilges, M.; Pannu, N. S.; Read, R. J.; Rice, L. M.; Simonson, T.; Warren, G. L. *Acta. Crystallogr., Sect. D: Biol. Crystallogr.* **1998**, *54* (Pt 5), 905.
(23) Read, R. J. *Acta Crystallogr., Sect. A* **1986**, *42*, 140.
(24) Brunger, A. T. *Acta. Crystallogr., Sect. D: Biol. Crystallogr.* **1993**, *49*, 24.
(25) Chen, V. B.; Arendall, W. B., 3rd; Headd, J. J.; Keedy, D. A.; Immormino, R. M.; Kapral, G. J.; Murray, L. W.; Richardson, J. S.; Richardson, D. C. *Acta. Crystallogr., Sect. D: Biol. Crystallogr.* **2010**, *66*, 12.
(26) Morris, G. M.; Goodsell, D. S.; Halliday, R. S.; Huey, R.; Hart, W. E.; Belew, R. K.; Olson, A. J. *J. Comput. Chem.* **1998**, *19*, 1639.
(27) Case, D. A.; Cheatham, T. E., III; Darden, T.; Gohlke, H.; Luo, R.; Merz, K. M., Jr; Onufriev, A.; Simmerling, C.; Wang, B.; Woods, R. *J. Comput. Chem.* **2005**, *26*, 1668.
(28) Cornell, W. D.; Cieplak, P.; Bayly, C. I.; Gould, I. R.; Merz, K. M., Jr; Ferguson, D. M.; Spellmeyer, D. C.; Fox, T.; Caldwell, J. W.; Kollman, P. A. *J. Am. Chem. Soc.* **1995**, *117*, 5179.
(29) Hornak, V.; Abel, R.; Okur, A.; Strockbine, B.; Roitberg, A.; Simmerling, C. *Proteins* **2006**, *65*, 712.
(30) Jorgensen, W. L.; Chandrasekhar, J.; Madura, J. D.; Impey, R. W.; Klein, M. L. *J. Chem. Phys.* **1983**, *79*, 926.
(31) Cornell, W. D.; Cieplak, P.; Bayly, C. I.; Kollman, P. A. *J. Am. Chem. Soc.* **1993**, *115*, 9620.
(32) Darden, T. A.; York, D.; Pedersen, L. *J. Chem. Phys.* **1993**, *98*, 10089.
(33) Essmann, U.; Perera, L.; Berkowitz, M. L.; Darden, T.; Lee, H.; Pedersen, L. *J. Chem. Phys.* **1995**, *103*, 8577.
(34) Ryckaert, J. P.; Ciccotti, G.; Berendsen, H. J. *J. Comput. Phys.* **1977**, *23*, 327.
(35) Shao, Y. et al. *Q Chem.*; Q. Chem, Inc.: Pittsburgh, PA, 2006
(36) Ponder, J. W. *Tinker*; Calculate Ltd.: St. Petersburgh, Russian Federation, 2004.
(37) Zhang, Y.; Lee, T.; Yang, W. *J. Chem. Phys.* **1999**, *110*, 46.
(38) Zhang, Y.; Liu, H.; Yang, W. *J. Chem. Phys.* **2000**, *112*, 3483.
(39) Torrie, G. M.; Valleau, J. P. *J. Comput. Phys.* **1977**, *23*, 187.
(40) Berendsen, H. J. C.; Postma, J. P. M.; van Gunsteren, W. F.; DiNola, A.; Haak, J. R. *J. Chem. Phys.* **1984**, *81*, 3684.
(41) Kumar, S.; Bouzida, D.; Swendsen, R. H.; Kollman, P. A.; Rosenberg, J. M. *J. Comput. Chem.* **1992**, *13*, 1011.
(42) Ke, Z.; Guo, H.; Xie, D.; Wang, S.; Zhang, Y. *J. Phys. Chem. B* **2011**, *115*, 3725.
(43) Linsky, T.; Fast, W. *Biochim. Biophys. Acta* **2010**, *1804*, 1943.
(44) Linsky, T. W.; Fast, W. Guanidine-Modifying Enzymes in the Pentein Superfamily; In *Comprehensive Natural Products II Chemistry and Biology*; Mander, L., Liu, H.-W., Eds.; Elsevier: Oxford, U.K., 2010; Vol. 8; p 125.
(45) *MARVIN 5.2.0*; ChemAxon: Budapest, Hungary, 2009.
(46) Stone, E. M.; Schaller, T. H.; Bianchi, H.; Person, M. D.; Fast, W. *Biochemistry* **2005**, *44*, 13744.
(47) Forbes, S. P.; Druhan, L. J.; Guzman, J. E.; Parinandi, N.; Zhang, L.; Green-Church, K. B.; Cardounel, A. J. *Biochemistry* **2008**, *47*, 1819.
(48) Linsky, T. W.; Monzingo, A. F.; Stone, E. M.; Robertus, J. D.; Fast, W. *Chem. Biol.* **2008**, *15*, 467.
(49) Livers, M.; Miller, J. *J. Chem. Soc.* **1963**, 3486.
(50) Reinheimer, J. D.; Gerig, J. T.; Garst, R.; Schrier, B. *J. Am. Chem. Soc.* **1962**, *84*, 2770.
(51) Stone, E. M.; Costello, A. L.; Tierney, D. L.; Fast, W. *Biochemistry* **2006**, *45*, 5618.